Available online at www.sciencedirect.com
SCIENCE DIRECT®
Tectonophysics 381 (2004) 61–79
TECTONOPHYSICS
www.elsevier.com/locate/tecto

Numerical modelling of the thermal evolution of the northwestern Dniepr–Donets Basin (Ukraine)

V.A. Shymanovskyy[a,b], R.F. Sachsenhofer[a,*], A. Izart[c], Y. Li[c]

[a] *Institut für Geowissenschaften, Montanuniversität Leoben, Peter-Tunner-Strasse 5, A-8700 Leoben, Austria*
[b] *Technological Centre of Ukrgeofisika, S. Perofska str. 10, UA-03057 Kyiv, Ukraine*
[c] *UMR 7566G2R, Université Henri Poincaré, BP239, F-54506, Vandoeuvre-les-Nancy, France*

Received 20 December 2001; accepted 8 August 2002

Abstract

The Dniepr–Donets Basin (DDB) is a Late Devonian rift structure located within the East-European Craton. Numerical heat flow models for 13 wells calibrated with new maturity data were used to evaluate temporal and lateral heat flow variations in the northwestern part of the basin.

The numerical models suggest that heat flow was relatively high during Late Carboniferous and/or Permian times. The relatively high heat flow is probably related to an Early Permian re-activation of tectonic activity. Reconstructed Early Permian heat flow values along the axial zone of the rift are about 60 mW/m^2 and increase to 90 mW/m^2 along the northern basin margin. These values are higher than those expected from tectonic models considering a single Late Devonian rifting phase. The calibration data are not sensitive to variations in the Devonian/Carboniferous heat flow. Therefore, the models do not allow deciding whether heat flows remained high after the Devonian rifting, or whether the reconstructed Permian heat flows represent a separate heating event.

Analysis of the vitrinite reflectance data suggest that the northeastern Dniepr–Donets Basin is characterised by a low Mesozoic heat flow (30–35 mW/m^2), whereas the present-day heat flow is about 45 mW/m^2.

Keywords: Heat flow; Dniepr–Donets Basin; Syn-rift phase; Post-rift phase; Thermal evolution; Basin modelling; Biomarker; Vitrinite reflectance

1. Introduction

During the last decade, the Pripyat–Dniepr–Donets (PDD), a Late Devonian rift structure located within the southern part of the East-European Craton, was the focus of extensive geological and geophysical research (Chekunov, 1994; Stephenson et al., 1996, 1999). New data and concepts contributed significantly to the understanding of the basin, which contains syn-rift sediments up to 4 km thick and post-rift sediments in excess of 15 km. Various numerical models were applied to assess the basin evolution quantitatively. These models used different approaches and stressed either thermal (Galushkin and Kutas, 1995; Sachsenhofer et al., 2002) or tectonic processes (van Wees et al., 1996; Kusznir et al., 1996a,b; Poplavskii et al., 2001), or a combination of both (Starostenko et al., 1999).

* Corresponding author. Tel.: +43-3842-402-788; fax: +43-3842-402-9902.
E-mail address: sachsenh@unileoben.ac.at (R.F. Sachsenhofer).

0040-1951/$ - see front matter © 2004 Elsevier B.V. All rights reserved.
doi:10.1016/j.tecto.2003.10.013

Most tectonic models consider a single Devonian (to Tournaisian) rifting phase and explain the huge thickness of the post-Devonian post-rift sequence by the rift-induced thermal anomaly. However, van Wees et al. (1996) have shown that in the Dniepr–Donets Basin (DDB; central part of the PDD) additional Early Carboniferous and Early Permian re-activation phases have to be considered in order to model the observed post-rift subsidence correctly. The different models of basin formation predict different thermal histories. Therefore, tectonic models can be tested for their plausibility using reconstructed heat flow histories.

In the present paper, we apply the basin modelling approach (Yalcin et al., 1997) to reconstruct the thermal history of 13 deep wells in the northwestern part of the DDB. The thermal histories are calibrated with new maturity depth trends. Apart from vitrinite reflectance, which is the most important maturity parameter, we determined the temperature of maximum hydrocarbon generation during pyrolysis (T_{max}; Espitalié et al., 1977) and biomarker ratios. Besides the tectonic aspects, the thermal basin evolution also has significance for the petroleum potential of the DDB, which hosts the largest hydrocarbon deposits in the Ukraine.

2. Geological setting

The DDB forms the central segment of the PDD Depression located in the southern part of the East European Platform. The PDD strikes in a northwestward direction over a distance of approximately 2000 km. Its width varies between 60 and 70 km in the northwest and 140 to 160 km in the southeast. Two Precambrian basement massifs bound this rift system: the Ukrainian Shield in the south and the Voronezh Massif in the north (Fig. 1). The DDB continues northwestward into the relatively shallow Pripyat Trough and southeastward into the inverted and

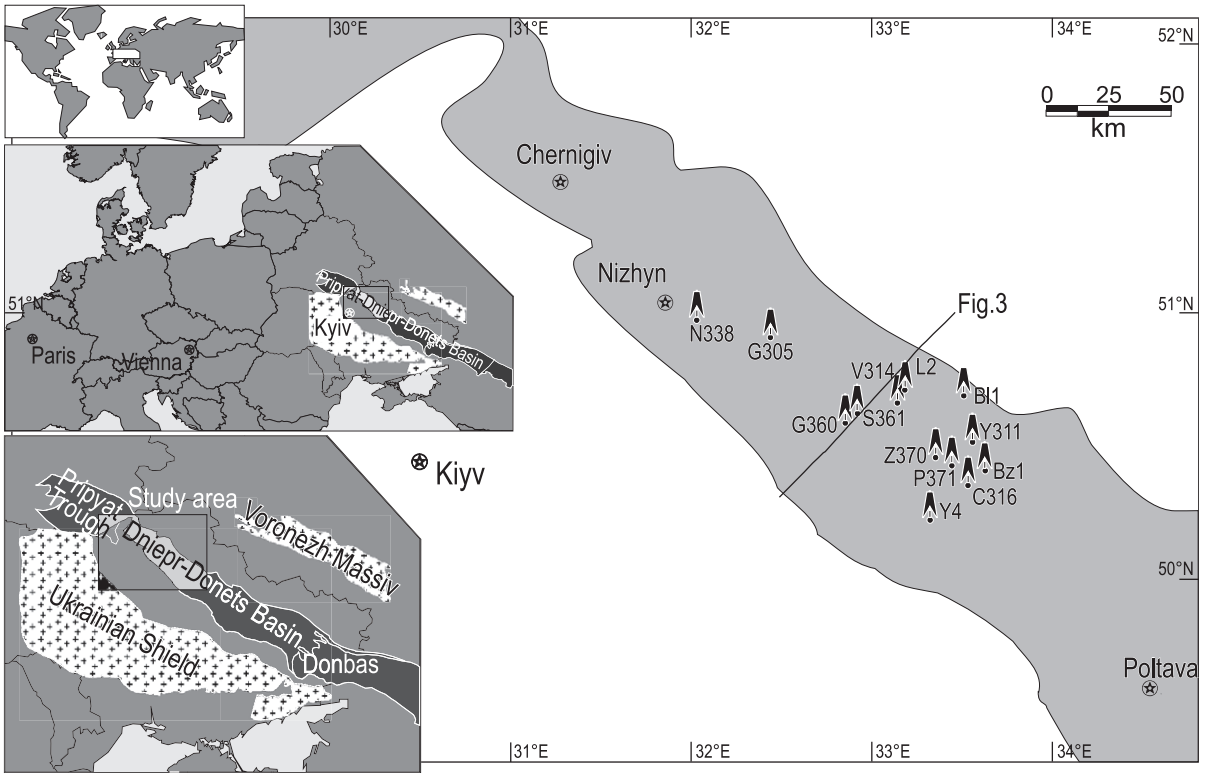

Fig. 1. Map showing the location of the study area and of the modelled wells in the Dniepr–Donets Basin.

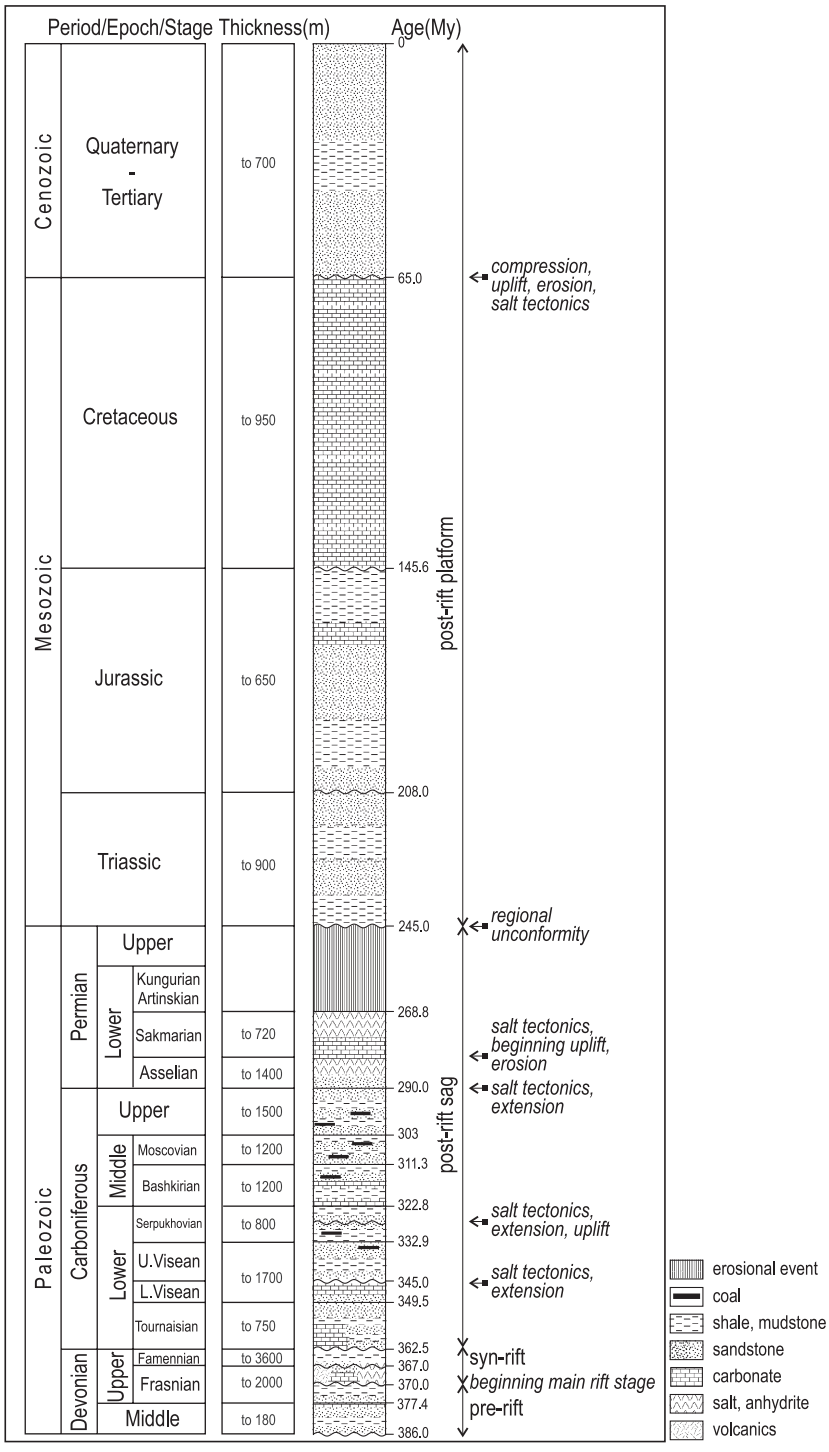

Fig. 2. Chrono- and lithostratigraphy of the Dniepr–Donets Basin. Major tectonic events are also shown (Vitenko et al., 1970; Ulmishek et al., 1994; Stovba et al., 1996; Ivanyuta et al., 1998). Time-scale after Harland (1990).

folded Donbas area. Inversion in the Donbas area occurred either during Permian (Privalov et al., 1998) or during Latest Cretaceous–Early Tertiary times (Stovba and Stephenson, 1999).

Chronostratigraphy and lithostratigraphy of the DDB are shown together with some major tectonic events in Fig. 2. The main rifting stage occurred during the Late Frasnian and Famennian stages and was accompanied by extensive igneous activity (Lyashkevich, 1987; Wilson and Lyashkevich, 1996). The total thickness of the Devonian succession including up to 3 km thick beds of salt, varies along the basin's strike from a few hundred meters to more than 4 km.

The post-rift phase is characterised by the formation of a vast syncline overlapping the rift shoulders. Carboniferous to Cenozoic rocks cover the rift flanks and increase in thickness towards the rift axis (Fig. 3). Ulmishek et al. (1994) subdivided the thick post-rift strata into a post-rift sag and a post-rift platform sequence. The boundary is defined by a regional pre-Triassic unconformity. According to Stephenson et al. (2001), the major unconformity results from a general sea level fall, an absolute uplift of the Eastern European platform and a monoclinal uplift of the southern basin margin. The latter is probably related to transtension rather than to compression, although minor reverse faults can be identified (Stovba and Stephenson, 1999). Several extensional or transtensional tectonic events had affected the DDB already during Carboniferous to Early Permian times (Stovba et al., 1996; Stephenson et al., 2001; Fig. 2). These tectonic events triggered salt movements, which commenced in the Late Devonian–Early Carboniferous (Chirvinskaya and Sollogub, 1980; Kivshik et al., 1991; Chekunov et al., 1992; Stovba and Stephenson, 2003) and reached a climax when Devonian salt reached the paleosurface during the Early Permian (Kivshik et al., 1993b), a time characterised by basin inversion according to Milanovsky (1992). A compressional event resulting in uplift and erosion occurred at the end of the Cretaceous period.

Carboniferous strata comprise clastics, thin limestone beds and coal. Lower Permian levels are characterised by evaporitic rocks and carbonates. The total thickness of the rocks representing the post-rift sag stage reaches 13 km, with the maximum depth of their base at about 15 km (Kivshik et al., 1993a,b). The post-rift platform sequence includes marine and terrestrial clastics and carbonates. Its thickness is significantly controlled by salt tectonics.

There are very few published maturity data from the DDB. Ivanova et al. (in Shpak, 1989) show a map of vitrinite reflectance values measured in air for a depth of 5 km. This map is reproduced in Ulmishek et al. (1994) with vitrinite reflectance in air transformed into vitrinite reflectance in oil. Shpak (1989) also reports present-day formation temperatures. According to this author, geothermal gradients are below 3 °C/100 m in the central and northwestern axial zone of the basin and increase toward the basin margins. Heat flow in the DDB ranges from 33 to 72 mW/m^2 (Hurtig et al., 1992) with average values of 44 mW/m^2 in the northwestern part of the DDB and 56 mW/m^2 in the Donbas area.

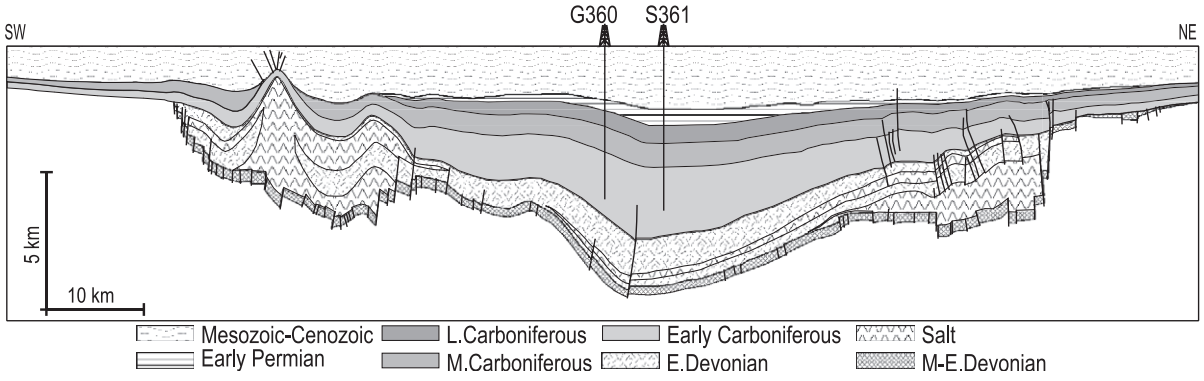

Fig. 3. Cross-section through the northwestern Dniepr–Donets Basin, based on a depth-converted reflection-seismic line (modified after Kivshik et al., 1993a). For location, see Fig. 1.

3. Samples and methods

3.1. Maturity parameters

About 140 core samples were taken from 13 wells in the northwestern part of the DDB (Fig. 1). Most samples are from Lower Carboniferous levels. Material from sediments younger than Bashkirian (lower Middle Carboniferous) was not available.

Vitrinite reflectance for these sediments was determined following established procedures (Taylor et al., 1998). Results are presented as mean random reflectance values (%R_r).

Rock Eval pyrolysis (Espitalié et al., 1977) was performed in duplicate. Here, only the maturity parameter T_{max} (temperature [°C] at which a maximum of hydrocarbons is formed during pyrolysis) is reported. Following suggestions by Peters (1986), T_{max} values from samples with S2 peaks below 0.2 mg HC/g rock were not considered.

Immature to marginally mature samples from three key wells (N338, G360, Z370) were selected for the determination of biomarker ratios (20*S*/[20*S*+20*R*] steranes, 22*S*/[22*S*+22*R*] hopanes, e.g. Mackenzie, 1984). The powdered rocks were extracted by chloroform at 60 °C for 45 min. The total extract obtained was fractionated by liquid chromatography into saturates, aromatics and polars. Saturates were analysed by gas chromatography–mass spectrometry using a HP 5890 II gas chromatograph and a HP 5971 mass selective detector. Hopanes were characterised after fullscan and SIM of $m/z=191$. Steranes were characterised after fullscan and SIM of $m/z=217$.

3.2. Thermal modelling

PDI-1D™ software of IES, Jülich (Wygrala, 1988) was used for modelling thermal histories. Input data include the thickness of stratigraphic units, the physical properties of their lithologies and the temporal evolution of the heat flow at the base of the sedimentary sequence, and of the temperature at the sediment–water interface. Detailed information on the stratigraphy and lithology of the modelled wells was provided by the Chernigiv State Geological Survey and the Chernigiv Branch of the Ukrainian State Geological Institute. Information on the thicknesses of strata eroded during Late Permian times was taken from Stovba et al. (1996) and Kabyshev et al. (1998). Middle Triassic to Early Jurassic times are considered a time of non-deposition in most wells, although there is some evidence for an angular unconformity between Triassic and Jurassic deposits (Stephenson et al., 2001 cum lit.). Physical parameters for different lithologies pre-defined in the software were used (Table 1) and the applied timescale follows Harland (1990).

The above information was used to reconstruct decompacted subsidence histories and the temperature field through time. The models were calibrated by modifying the heat flow until a satisfactory fit between measured and calculated formation temperatures, vitrinite reflectance and biomarker ratios (sterane- and hopane-isomerisation) was obtained. Published heat flow scenarios (Starostenko et al., 1999) considering heat flow variations associated with Devonian rifting were used as a starting point. However, an additional thermal event had to be

Table 1
Physical properties assigned to standard lithotypes used for simulations

Lithotype	Density (kg/m^3)	Initial porosity	Compress (Pa^{-1})		Matrix thermal conductivity (W/m K)		Heat capacity (cal/g K)		Permeability[a] at porosity of	
			Max.	Min.	20 °C	100 °C	20 °C	100 °C	5%	75%
Water	1160	0	2	1	0.60	0.68	0.999	1.008	1.0	1.0
Sandstone	2660	42	500	10	3.12	2.64	0.178	0.209	−2.0	0.0
Siltstone	2672	56	8000	10	2.14	2.03	0.201	0.242	−5.0	0.0
Mudstone	2680	65	60000	10	1.98	1.91	0.213	0.258	−5.5	−1.0
Limestone	2710	42	300	25	2.83	2.56	0.195	0.223	−4.0	13.0
Evaporite	2540	10	1	10	4.69	3.91	0.194	0.210	−16.0	−16.0
Coal	2000	52	130000	10	0.50	0.46	0.204	0.248	−5.5	−1.0
Donbas, Suite N	2664	56	26178	10.2	2.35	2.15	0.199	0.239	−5.25	−0.26

[a] Permeabilities (−5 means 10^{-5} md) are calculated for different stages of porosity.

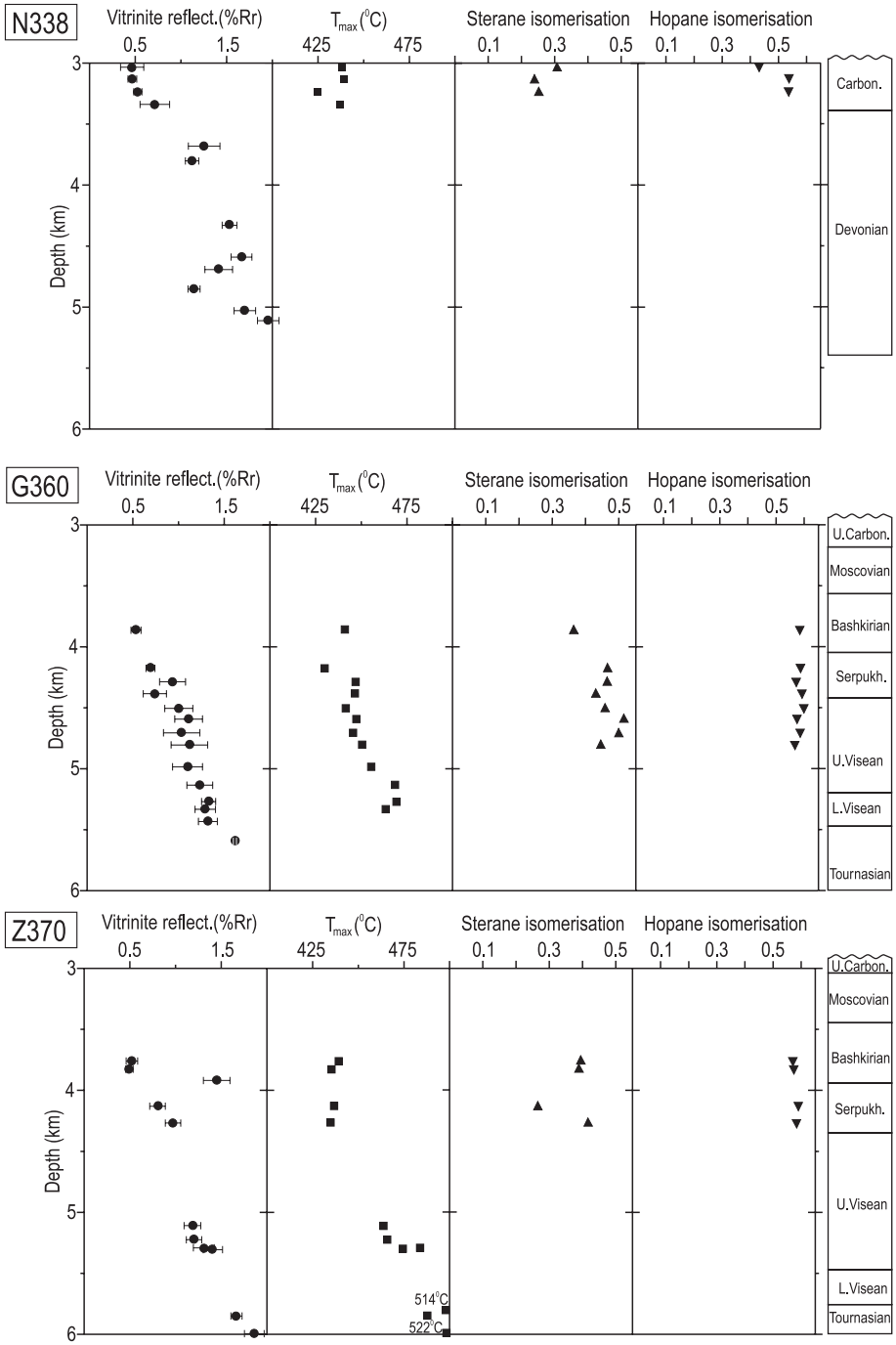

Fig. 4. Vitrinite reflectance, T_{max}, strerane and hopane isomerisation for key wells in the northwestern Dniepr–Donets Basin.

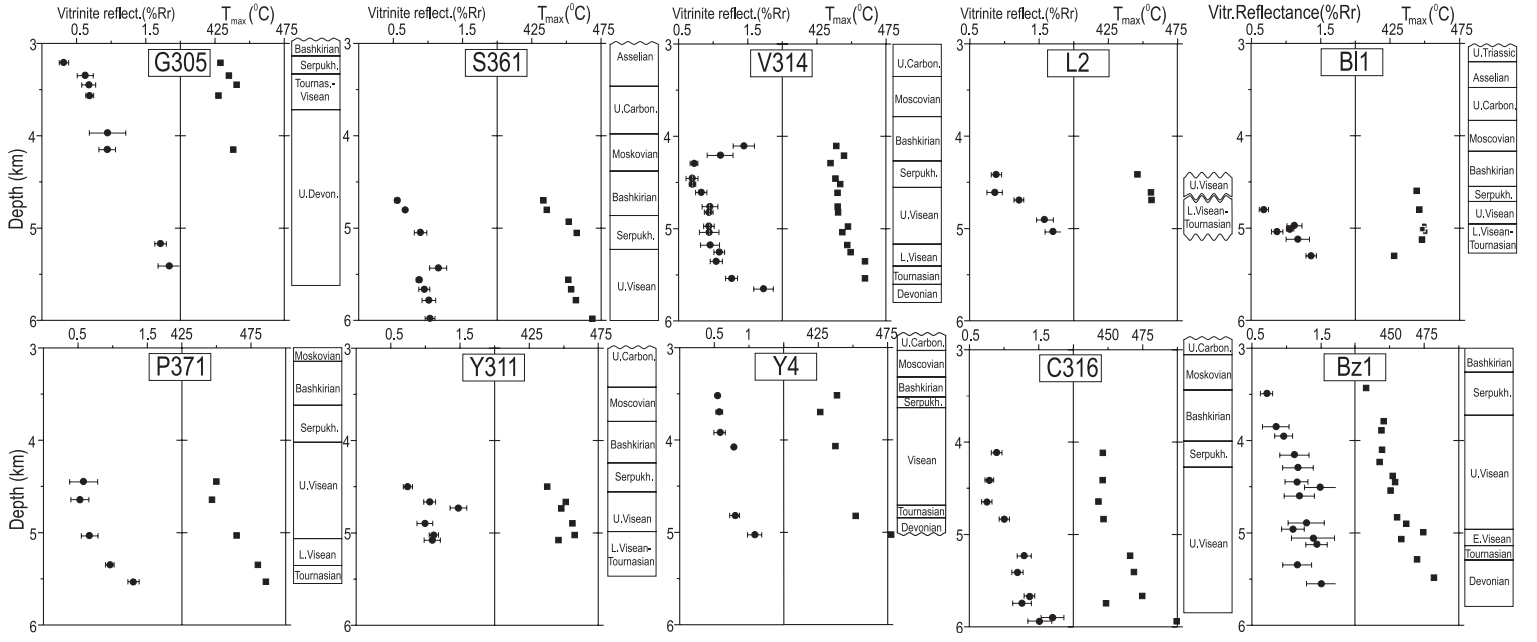

Fig. 5. Vitrinite reflectance and T_{max} for wells in the northwestern Dniepr–Donets Basin.

included to obtain a good calibration. Early Carboniferous and Early Permian extensional re-activations occurred during the post-rift stage, whereas the Mesozoic history was marked by tectonic quiescence (Stovba et al., 1996). Therefore, Early Carboniferous or Early Permian heat flow events appear more plausible than a Mesozoic event. The studied Lower Carboniferous rocks were near the surface during Early Carboniferous time. Consequently, a possible Early Carboniferous heating event had little influence on the calibration data. Hence, an Early Permian heat flow event was considered in our conceptual model.

Vitrinite reflectance was calculated using the kinetic EASY% Ro approach (Sweeney and Burnham, 1990). Biomarker ratios were calculated using kinetic data from Rullkötter and Marzi (1988). Because vitrinite reflectance and biomarker ratios are mainly controlled by maximum temperatures, only heat flows around times of maximum temperatures can be determined precisely.

4. Results

4.1. Maturity

Maturity trends for the depth intervals from 3 to 6 km are shown in Figs. 4 and 5. Vitrinite reflectance varies from 0.4% to 2.0% R_r and T_{max} ranges between 420 and 520 °C. Sterane isomerisation ratios are 0.2–0.55. Hopane ratios for wells G360 and Z370 reached equilibrium (0.6), but are lower in well N338 (0.42–0.55).

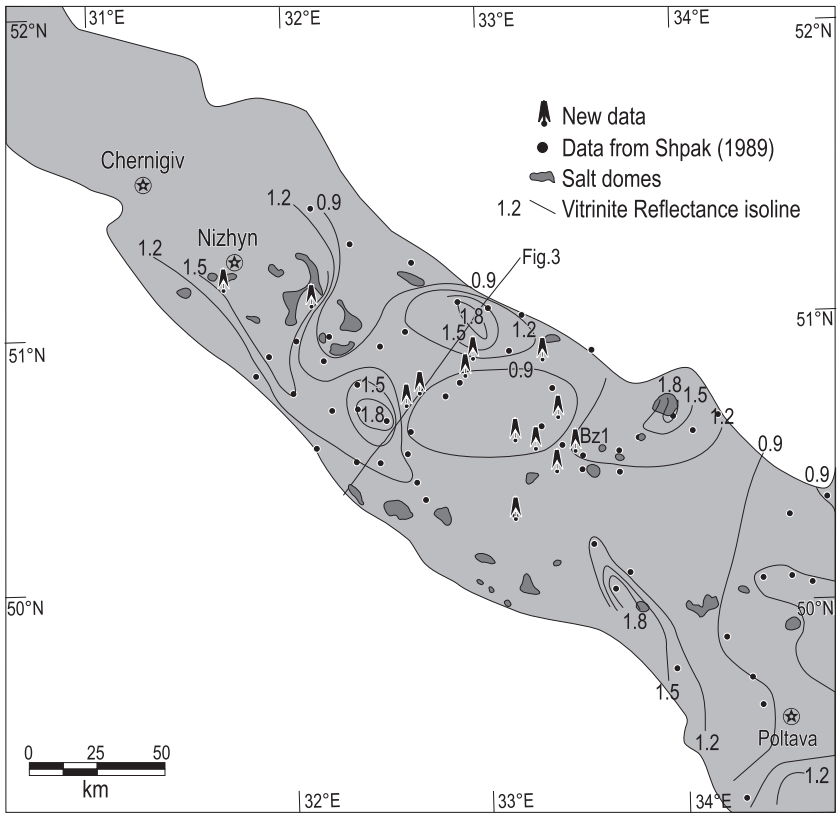

Fig. 6. Hand-contoured map showing vitrinite reflectance (%R_r) at the depth of 5 km below sea level. The position of salt domes is indicated (Dvoryanin et al., 1987). This maturity map considers data from Shpak (1989) (reflectances in air were recalculated to those in oil after Ammosov et al., 1977) and our new data.

There is a considerable scatter in vitrinite reflectance and T_{max} data in some wells. This is due in part because outliers (e.g. shallow samples in well V314, Fig. 5) were not eliminated to avoid data manipulation. A wide scatter of reflectance data also occurs in the Devonian section of well N338 (Fig. 4). Unfortunately, because of tiny S2 peaks, T_{max} values cannot be used to support reflectance data for this well. Well S361 shows a sharp downward decrease in reflectance data at 5.5 km depth, but no indication for a tectonic explanation (e.g. reverse fault) is present from the well log or regional seismic lines (Fig. 3).

The regional distribution of vitrinite reflectance at a depth of 5 km is shown as a map in Fig. 6. Rocks from the Devonian to the Middle Carboniferous are found at this depth (see also Ulmishek et al., 1994). The hand-contoured map considers reflectance values of Shpak (1989) and our new data. The map indicates that lowest values are found in the axial zone of the DDB, while the highest values occur along the basin margins.

There are no maturity data from Mesozoic rocks. However, low maturity in Bashkirian rocks suggest that vitrinite reflectance within the Mesozoic section is significantly below 0.5%.

4.2. Paleoheat flow

4.2.1. Heat flow scenarios

Different heat flow scenarios were applied to the numerical models of wells G360, Z370 and N338 (Fig. 7). The resulting calculated temperature, vitrinite reflectance and biomarker data are shown in Fig. 8. Fig. 9 summarises the temporal evolution of temperature, vitinite reflectance and biomarker ratios for lower Visean and Bashkirian horizons in well G360 for the different heat flow scenarios.

As a starting point, we used a heat flow model proposed by Starostenko et al. (1999, their model 1b, scenario 1). This model assumes a Devonian asthenospheric upwelling to a depth of 50 km. The temperature of the asthenospheric upwelling was held constant (1200 °C) during the entire rifting period (10 m.y.). The model is characterised by a Devonian heat flow maximum of 92 mW/m^2 and a rapid decrease to equilibrium values (30–35 mW/m^2) during the post-rift stage (for details, see Starostenko et al., 1999). Fig. 8 shows that this scenario results in a bad calibration and therefore had to be modified.

Heat flow scenario 2 differs from scenario 1 in considering a higher equilibrium heat flow (45 mW/m^2). It results in a good fit with measured temperature and vitrinite reflectance data, but considerably overestimates biomarker isomerisation. The application of an alternative kinetic data set for the calculation of biomarker isomerisation (Mackenzie and McKenzie, 1983) results in an even greater overestimation.

In order to avoid the overestimation of biomarker ratios, we returned to heat flow scenario 1 and increased the heat flow only since Cenozoic times to present-day levels. This heat flow scenario 3 results in a good fit with all calibration data, except vitrinite reflectance.

Heat flow scenario 4 introduces elevated heat flows (68–80 mW/m^2) during the known Early Permian (Asselian-Sakmarian) tectonic activity. It results in a good agreement with all calibration data in the key wells (Fig. 8), although vitrinite reflectance calculated for the uppermost part of the Lower Carboniferous section is above the measured values. Note that the timing of the heat flow event is mainly

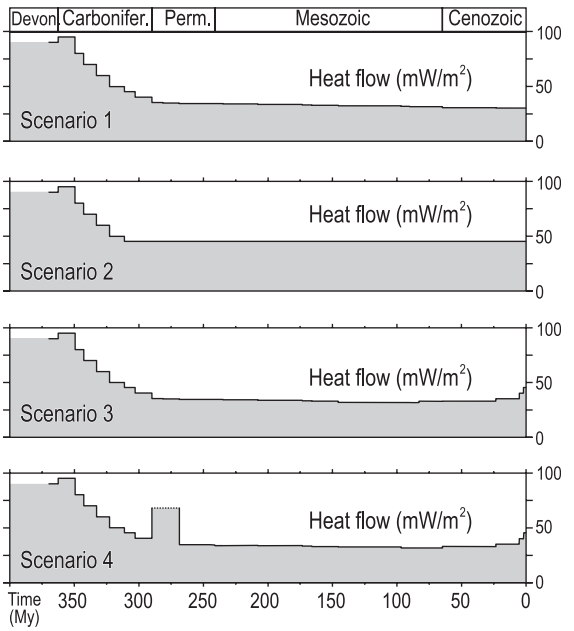

Fig. 7. Heat flow scenarios applied for key wells in the northwestern Dniepr–Donets Basin. A best fit between measured and calculated calibration data is obtained with scenario 4.

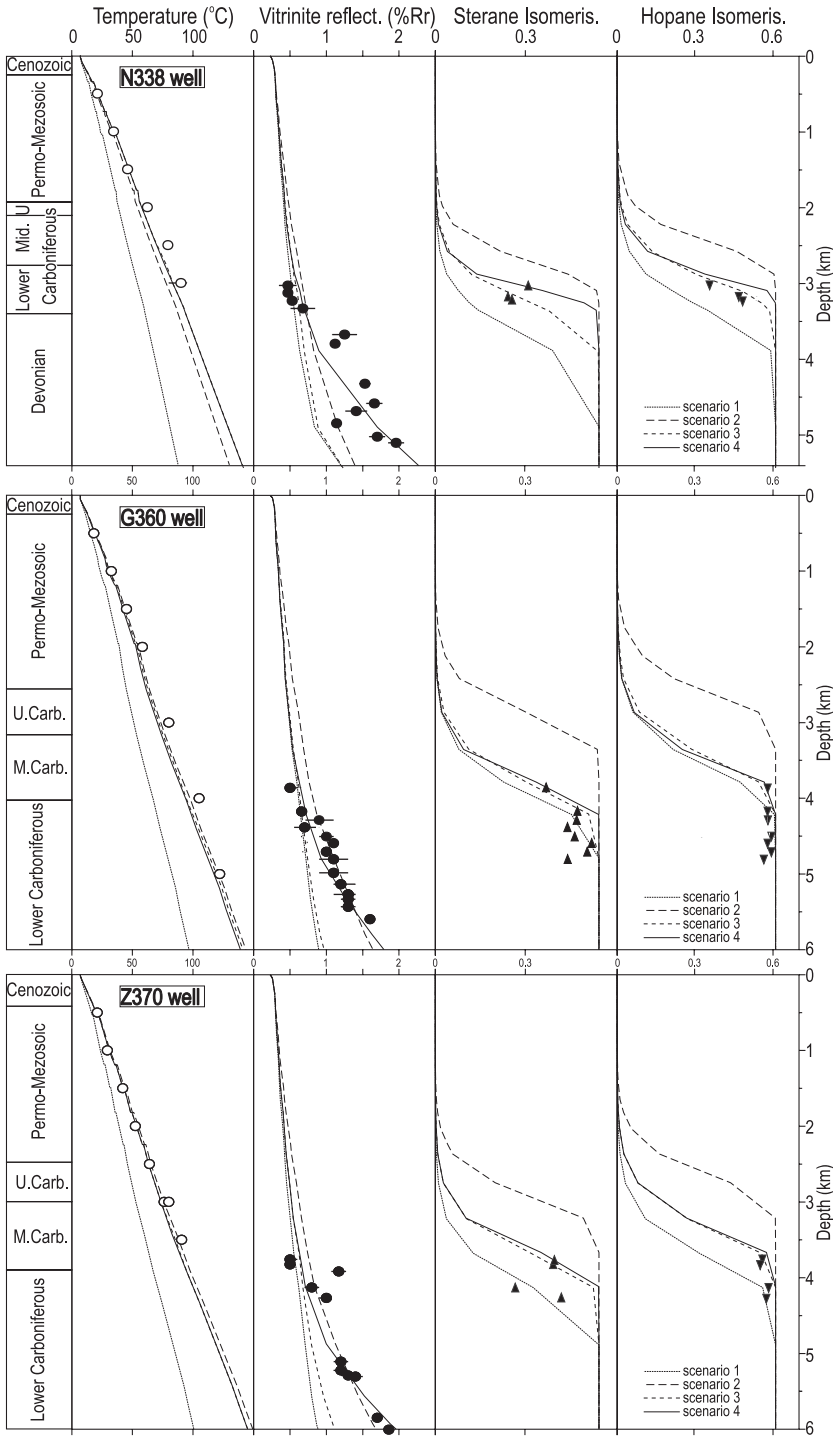

Fig. 8. Measured and calculated calibration data for key wells. Different lines refer to different heat flow scenarios shown in Fig. 7.

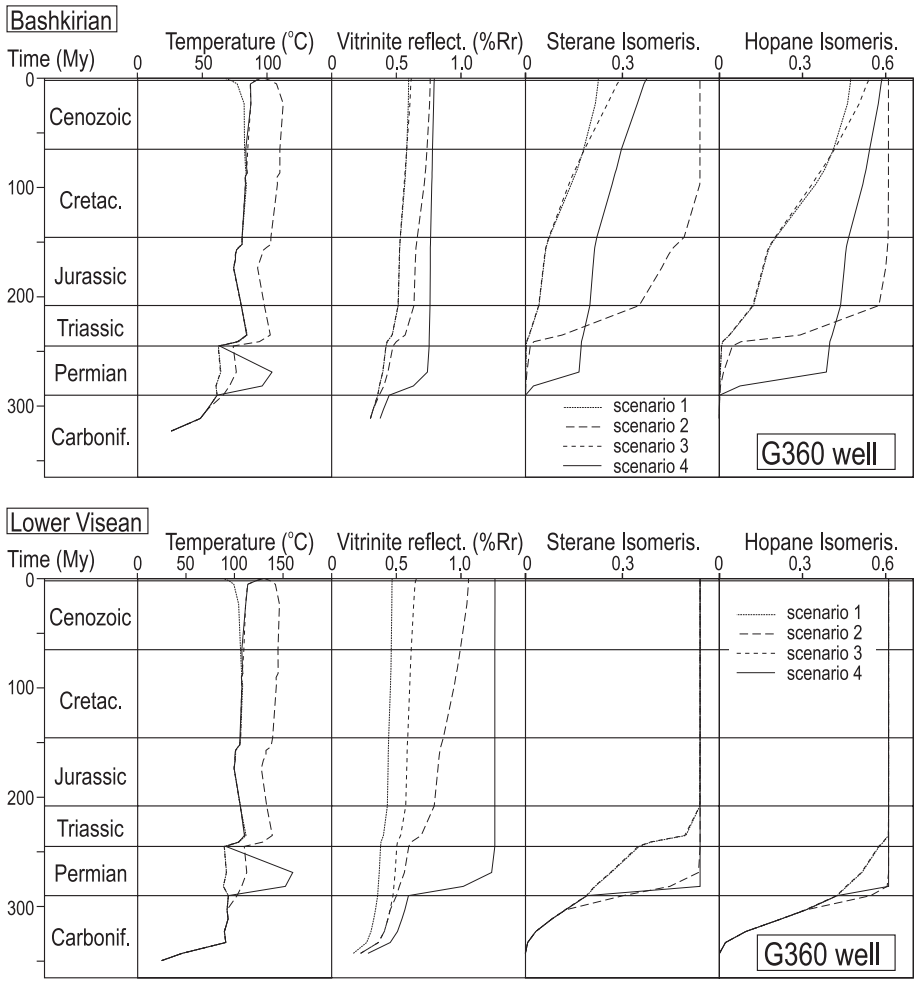

Fig. 9. Calculated temporal evolution of calibration data for Bashkirian and lower Visean horizons in key well G360.

based on geological arguments (Early Permian tectonic re-activation).

Nevertheless, scenario 4 was considered most likely and was applied to 10 additional wells. In these wells, a satisfactory calibration was obtained applying Early Permian heat flows between 60 and 90 mW/m^2 (Figs. 10 and 11).

4.2.2. Sensitivity analysis

Four groups of alternative models were introduced to check the sensitivity of the results.

(1) First, Early Permian heat flow was changed by ± 10%, which resulted in a poor calibration suggesting that the uncertainty of the heat flow estimates is within this order of magnitude (Figs. 10 and 11).

(2) Second, the physical properties of the rocks were modified. In the original model, standard siliciclastic and carbonate lithotypes are used. Carboniferous rocks in the northwestern DDB contain minor amounts of coal. Coaly material in sediments decreases bulk thermal conductivity. In order to test a possible influence on the modelling results, we changed the thermal properties of the Carboniferous sediments. Physical rock parameters, which were used in a recent study for Upper Carboniferous rocks in the Donbas area containing 0.4% coal (suite N in

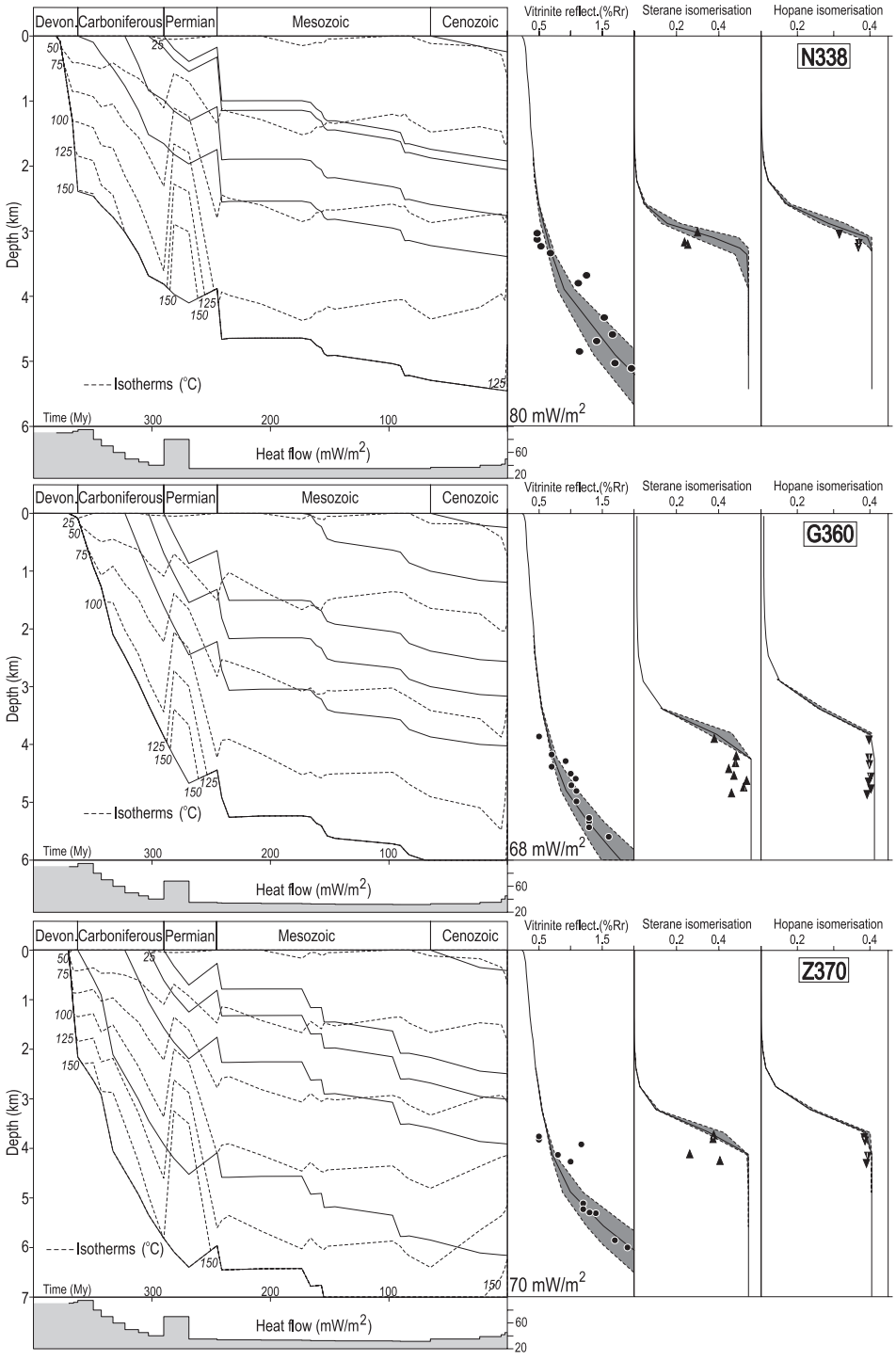

Fig. 10. Subsidence, temperature and heat flow histories (scenario 4) of key wells. On the right, measured (dots and triangles) and calculated (lines) calibration data are shown. Changing the original Early Permian heat flow by ± 10% results in a poor fit (dashed lines).

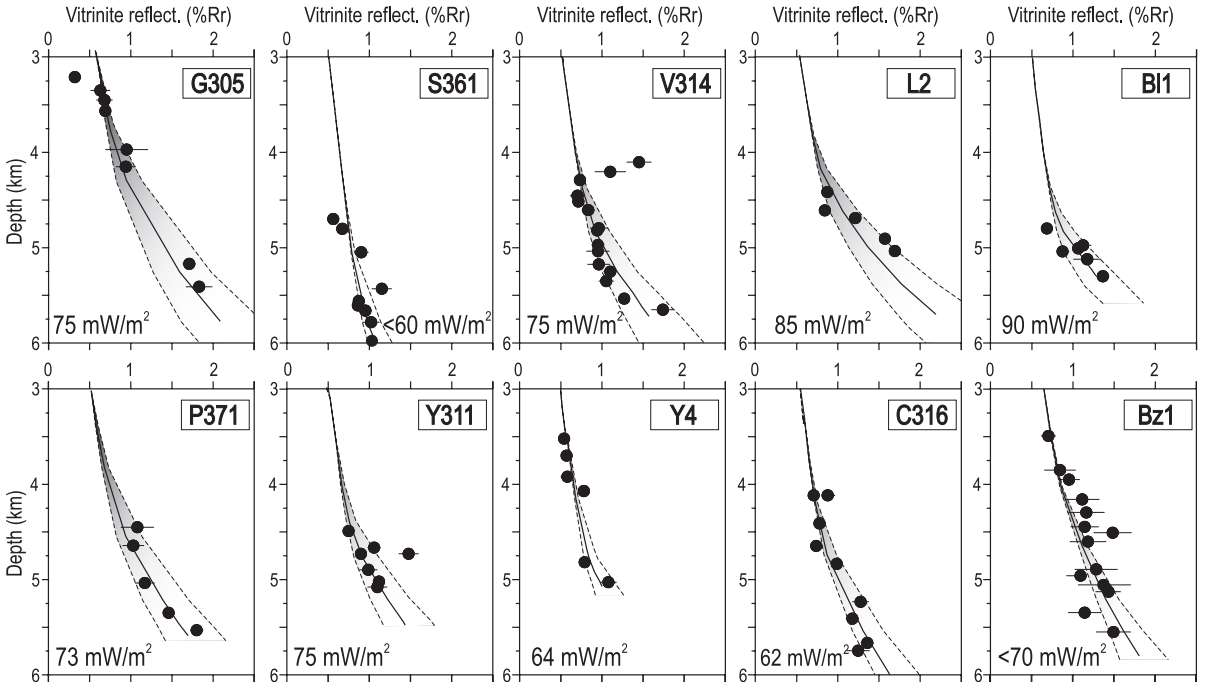

Fig. 11. Measured (dots) and calculated (lines) vitrinite reflectance (%R_r) for wells in the northwestern Dniepr–Donets Basin. Heat flow scenario 4 (Fig. 7) was applied to all wells. Values in the lower left corner of each box refer to Early Permian heat flows. Changing the original Early Permian heat flow by ± 10% results in the dashed lines.

Sachsenhofer et al., 2002), were used in the alternative model (see Table 1 for rock physical parameters). Although, the percentage of coal in the northwestern DDB is lower than in the Donbas, the results are influenced by less than 5%, suggesting that the content in coaly material has little effect on the model results.

(3) It has been noted that the Early Permian age of the heat flow event is mainly based on geological arguments. Therefore, in a third set of sensitivity analysis, the timing of the heat flow event was varied from Bashkirian to Late Triassic times to check the effect of different ages. Obviously, heat flow values also had to be adjusted in order to compensate the different burial depths during the heat flow events. As an example, calculated calibration data are presented for well G360 in Fig. 12. The figure illustrates that a shift of the heat flow event into Triassic times results in an overestimation of biomarker ratios. However, an Early Triassic event, although unlikely considering the geologic history, cannot be excluded based on the model alone. Note, that a possible pre-Middle Jurassic erosion event results in an even worse misfit. In any case, Jurassic to Cretaceous heat flow was only in the range of 30–35 mW/m^2.

A shift of the thermal event into Carboniferous times has little influence on biomarker data, but causes a change in calculated vitrinite reflectance trends (Fig. 12). The calculated reflectance curves applying Bashkirian (100 mW/m^2) or Moskovian (90 mW/m^2) heat flow events result in a slightly better fit with data from Lower Carboniferous rocks, but are characterised by a distinct increase in reflectance gradients below 4.7 km depth, which cannot be observed in the measured data.

These sensitivity models therefore show that thermal events between Late Carboniferous and Early Triassic times agree with the calibration data. However, geological reasons for elevated heat flow are known only from the Early Permian.

(4) Finally, we modified Devonian/Carboniferous heat flows and tested the alternative models using

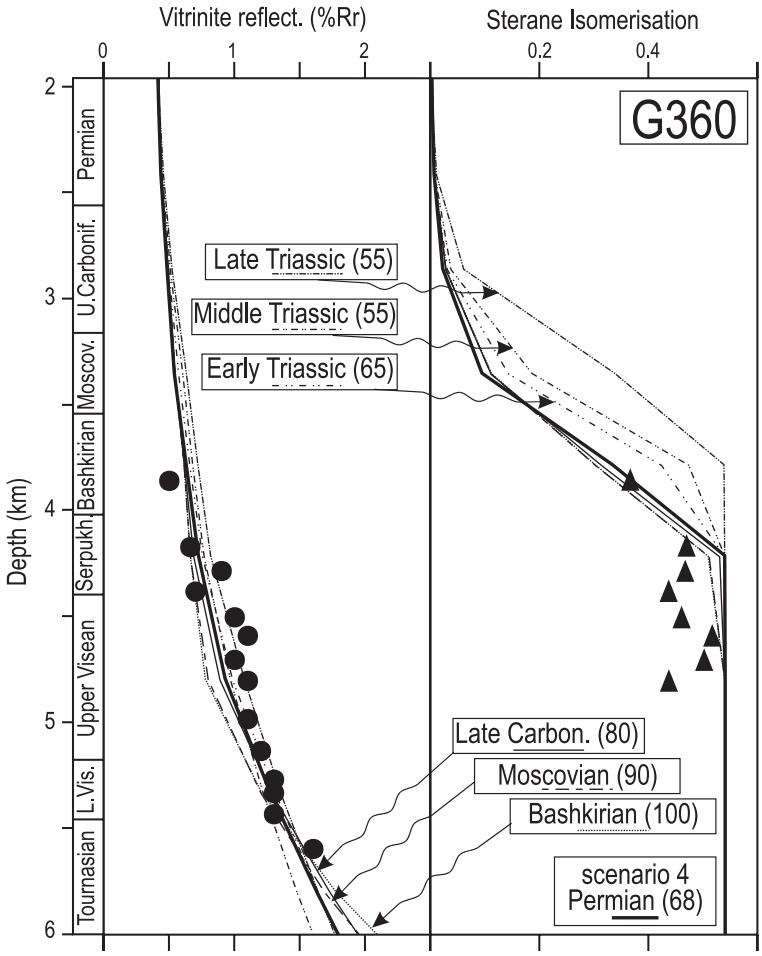

Fig. 12. Measured and calculated calibration data for well G360 applying heat flow events with different ages (see boxes). Numbers in brackets are heat flows during the thermal event in mW/m^2.

wells G305 and N338, where reflectance values from Devonian rocks cover a depth interval of more than 1.5 km (Fig. 13). The first model (scenario 5) considers a slow gradual heat flow decrease between Devonian and Permian time. Fig. 13 shows that this change has a negligible influence on the calibration data. Thereafter, a slowly decreasing Devonian syn-rift heat flow of 120 mW/m^2 was considered (scenario 6). Only in this case a minor change in calculated reflectance data can be observed. This shows that the calibration data are rather insensitive to pre-Permian heat flow variations and that it is impossible to distinguish between a separate Permian heat flow event (scenario 4) and the assumption that the heat flow remained high after Devonian rifting (Fig. 13).

5. Discussion

5.1. Influence of salt structures

Salt structures including up to 15 km thick salt domes are striking features within the DDB (Stovba and Stephenson, 1999, 2003). Salt has a very high thermal conductivity and can modify the temperature distribution in sedimentary basins (e.g. Mello et al., 1995). In particular, geothermal gradients and matu-

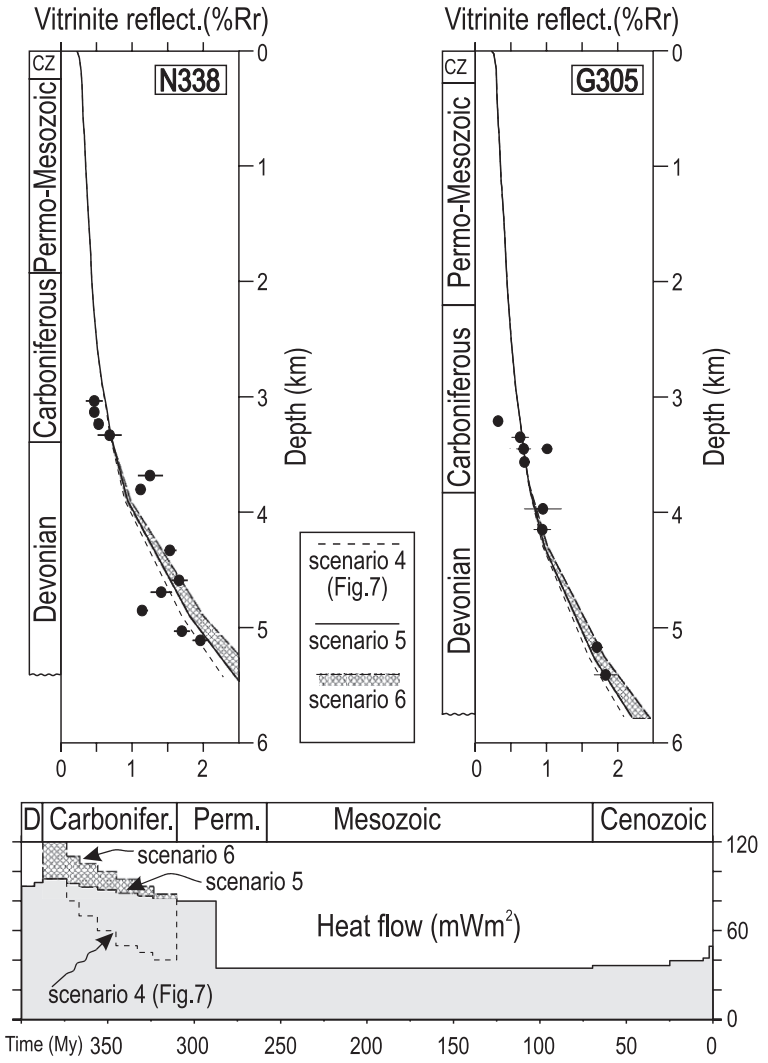

Fig. 13. Alternative Paleozoic heat flow models. The calculated vitrinite reflectance data show that the calibration data do not allow to distinguish between the different models.

rity above salt domes may be increased. It is therefore necessary to check if the observed maturity and the reconstructed heat flow histories are influenced by salt domes.

Fig. 6 shows the regional vitrinite reflectance pattern at a depth of 5 km. Several maxima with reflectance values above 1.8% R_r form prominent anomalies. The distribution of salt domes is also indicated in Fig. 6. Note that there is no systematic relation between reflectance anomalies and the location of salt domes, although the location of an anomaly northeast of well Bz1 coincides with a large salt dome. Fig. 6 also shows that most wells studied in the present paper are located far away from salt domes. Therefore, the observed reflectance trends and the reconstructed lateral and temporal heat flow variations are probably not influenced by salt.

5.2. Lateral distribution of Early Permian heat flow

The thermal models indicate elevated heat flows between Late Carboniferous and Early Triassic times.

Tectonic evidence (extension) suggests an Early Permian event. The regional distribution of reconstructed Early Permian heat flows is shown in Fig. 14. Reconstructed heat flow values are up to 90 mW/m^2. Maximum values occur along the northern margin of the DDB with heat flow isolines running approximately parallel to the basin margin. Minimum values are located along the basin axis.

Permian heat flow values from different parts of the DDB are presented in the insert of Fig. 14. Similar to wells in the northwestern DDB, well Suh3 southeast of Poltava is characterised by a moderate Early Permian heat flow (60 mW/m^2) and a low Mesozoic heat flow (35 mW/m^2; Sachsenhofer, 1999). The Permian heat flow value agrees with the position of the borehole close to the basin axis. Sachsenhofer et al. (2002) reconstructed heat flows during maximum burial during Permian times in the western part of the inverted Donets Basin (Donbas). Isolines are shown in the insert of Fig. 14. Note that during Permian times heat flow was generally lower (40–75 mW/m^2) in the Donbas than in the northwestern DDB. The 50 mW/m^2 isoline also runs parallel to the basin margin, but the 60 and 70 mW/m^2 isolines are perpendicular to it and follow a major tectonic lineament (Donetsk–Kadievka fault zone). This separates an area with moderate Permian erosion in the NW from an area with very high Permian uplift in the southeast (see Sachsenhofer et al., 2002 for details).

5.3. Implications for tectonic models

Models of the evolution of extensional basins predict that most of the thermal anomalies accompanying rifting vanish within a relatively short time-span of 50–70 m.y. (e.g. McKenzie, 1978; Allen and Allen, 1990; Kusznir et al., 1996a,b; Starostenko et al., 1999). The relatively high (Late Carboniferous?)

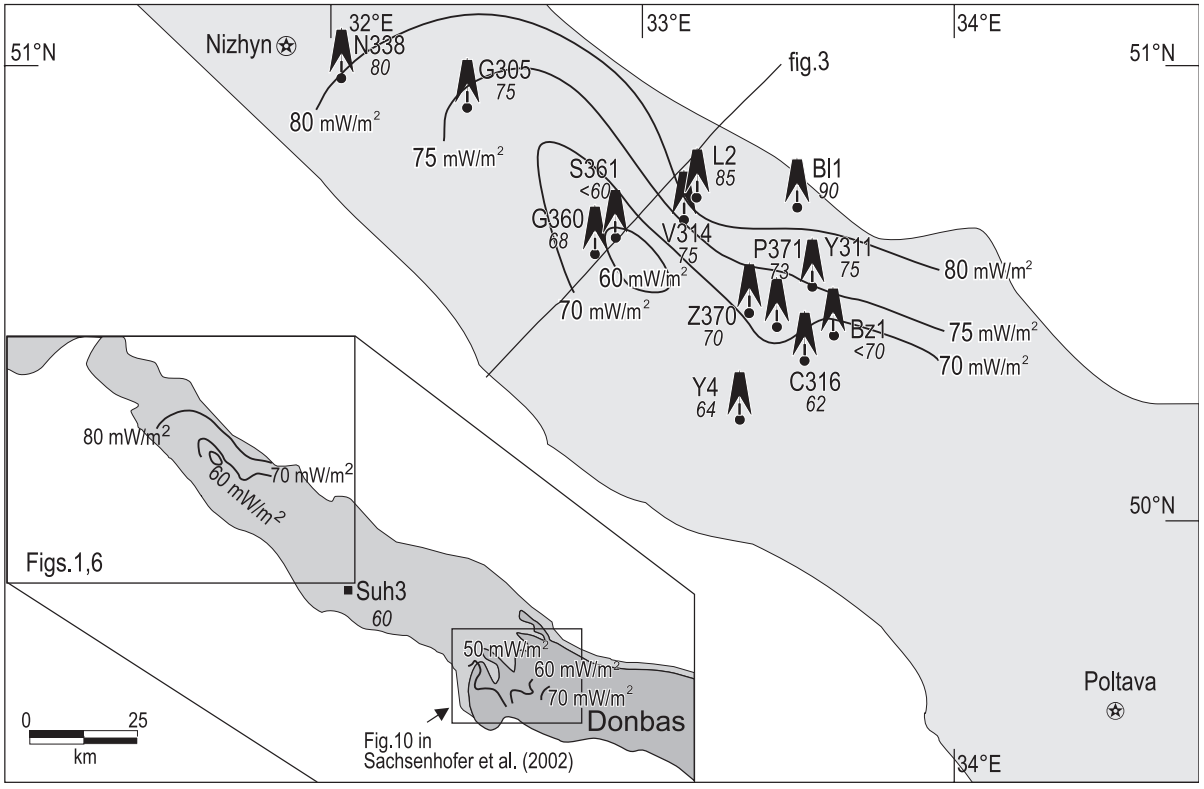

Fig. 14. Map showing the regional distribution of reconstructed Early Permian heat flows (numbers below well names) in the northwestern Dniepr–Donets Basin. Insert shows heat flow in the western Donbas area during Permian maximum burial (Sachsenhofer et al., 2002) and in the Poltava region (Suh3 well, Sachsenhofer, 1999).

Early Permian heat flow values reconstructed for the northwestern DDB do not agree with these models.

In the following, different processes which might be responsible for the observed Late Palaeozoic heat flow will be addressed. The discussion is complicated because our models do not distinguish between a separate (Late Carboniferous) Permian heating event (scenario 4, Fig. 7) and a continuous decrease in heat flow between Devonian and Permian time (alternative model, Fig. 13).

(1) Anomalous heat flow accompanying Devonian rifting: It is remarkable that the thickness of Devonian (Late Frasnian and Late Famennian) syn-rift volcanic rocks reaches a maximum in the northwestern DDB. According to Wilson and Lyashkevich (1996), magmatism was triggered by upwelling of a thermally (and geochemically) anomalous mantle plume. Perhaps, the mantle plume remained hot for an anomalously long time.

(2) Post-rift re-activations: An anomalous slow decrease in Carboniferous heat flow could also be related to post-rift re-activations during Visean, Serpukhovian and Early Permian times (Fig. 2, see also van Wees et al., 1996). Obviously, a separate heat flow event restricted to the (Late Carboniferous?) Early Permian cannot be ruled out according to the modelling results.

Note that models for the key wells suggest that heat flow decreased rapidly between Permo–Carboniferous and Triassic times in the northwestern DDB and that Mesozoic heat flow was rather low (30–35 mW/m^2). This is in contrast to the western Donbas area, where Sachsenhofer et al. (2002) reconstructed post-Early Permian thermal events, which are most probably related to Late Permian or Mesozoic magmatic intrusions. These variations highlight differences in the regional distribution of magmatism: syn-rift magmatic activity occurred in both segments of the PDD, but reached its maximum in the northwestern DDB, whereas post-rift magmatism was restricted to the Donbas area.

6. Conclusions

The applied numerical models suggest that Late Carboniferous/Permian heat flow in the northwestern DDB was relatively high. A Permian stretching phase indicates an Early Permian age of the heat flow event. Reconstructed Early Permian heat flows range from 60 to 90 mW/m^2 and increase from the axial zone of the northwestern DDB towards the basin margins. The reconstructed heat flow values are generally higher than those in the western Donbas. They are also significantly higher than those expected from lithospheric stretching and thermal subsidence models using a single Devonian rifting phase. However, from the thermal models alone, it is impossible to decide whether heat flow remained high after Devonian rifting, or whether the required Permian heating forms a separate heat flow event.

Low maturity values in the upper part of the Carboniferous sequence suggest that Mesozoic heat flow was only in the range of 30–35 mW/m^2. A Cenozoic increase in heat flow to present-day values ranging from 40 to 45 mW/m^2 is indicated by formation temperatures. Geological reasons for the recent increase in heat flow are not yet known.

Acknowledgements

Core samples and detailed information on stratigraphy and lithology of the studied wells were kindly provided by Chernigiv State Geological Survey, Chernigiv Branch of Ukrainian State Geological Institute and Ukrgeofizika, Kyiv. The paper benefited greatly from discussion with A.V. Ivanova, A.A. Kitchka, V.A. Krivosheya, T.M. Prigarina and colleagues involved in the GeoRift project of Europrobe, a program of the European Science Foundation. V.Sh. was supported by INTAS project 96-1701, AAPG Foundation and Austrian Exchange Service (ÖAD). Linguistic improvements by Charlotte Wohlfahrt are gratefully acknowledged. The paper benefited greatly from the critical remarks of C. Bueker and U. Bayer.

References

Allen, P.A., Allen, J.R., 1990. Basin Analysis: Principles and Applications. Blackwell, Cambridge. 451 pp.

Ammosov, I.I., Gorshkov, B.I., Grechishnikov, N.P., Kalmikov, G.S., 1977. Paleogeothermal Criteria of Distribution of Oil Fields (in Russian). Nedra, Moscow. 158 pp.

Chekunov, A.V., 1994. The geodynamics of the Dnieper–Donets rift syneclise (in Russian). Geophys. J. 16 (3), 3–13.

Chekunov, A.V., Gavrish, V.K., Kutas, R.I., Ryabchun, L.I., 1992. Dniepr–Donets paleorift. In: Ziegler, P.A. (Ed.), Geodynamics of Rifting: Vol. I. Case History Studies on Rifts: Europe and Asia. Tectonophysics, vol. 208, pp. 257–272.

Chirvinskaya, M.V., Sollogub, V.B., 1980. Deep Structure of the Dniepr–Donets Aulacogen from Geophysical Data (in Russian). Naukova Dumka, Kiev. 178 pp.

Dvoryanin, E.S., Samoilyuk, A.P., Smekalina, L.V., 1987. Structural Map of the Dniepr–Donets Depression. Scale 1:500 000. Ministry of Geology of the USSR.

Espitalié, J., Laporte, J.L., Madec, M., Marquis, F., Leplat, P.M., Paulet, J., Boutefeu, A.P., 1977. Méthode rapide de charactérisation des roches mères de leur potential petrolier et de leur degré d'evolution. Rev. Inst. Fr. Pét. 32, 23–43.

Galushkin, Yu.I., Kutas, R.I., 1995. The Dnieper–Donets palaeorift: evolution of the thermal regime and oil–gas potential. Geophys. J. 15, 335–352 (Overseas Publishers Assoc.).

Harland, W.B., 1990. A Geologic Time Scale 1989. Cambridge Univ. Press, Cambridge. 263 pp.

Hurtig, E., Cermak, V., Haenel, R., Zui, V., 1992. Geothermal Atlas of Europe. Hermann Haack Verlagsgesellschaft. Geographisch-Kartographische Anstalt, Gotha. 156 pp.

Ivanyuta, M.M., Fedyshyn, V.O., Denega, B.I., Arsiriy, Y.O., Lazaruk, Y.G., 1998. Atlas of Oil and Gas Fields of Ukraine. Six Volumes. Ukrainian Oil and Gas Academy, Lviv.

Kabyshev, B., Krivchenkov, B., Stovba, S., Ziegler, P.A., 1998. Hydrocarbon habitat of the Dniepr–Donets depression. Mar. Pet. Geol. 15, 177–190.

Kivshik, M.K., Samoiluk, A.P., Stovba, S.M., Turchanenko, M.T., 1991. Seismic–stratigraphic investigations—the base for building geodynamic model of the DDD. Abstr. Pap., 36th Int. Geophys. Symp., vol. 3, pp. 273–281. Kiev.

Kivshik, M.K., Stovba, S.M., Turchanenko, M.T., Redkolis, V.A., 1993a. The Regional Seismostratigraphic Investigations in the Dniepr–Donets Depression (in Russian). Ukrgeofisika, Kiev. 84 pp.

Kivshik, M.K., Stovba, S.M., Turchanenko, M.T., 1993b. Certain features of the Dniepr–Donets depression structure from the regional seismic–stratigraphic investigations data (in Russian). Geol. J. (Kiev) 2, 87–98.

Kusznir, N.J., Kovkhuto, A., Stephenson, R.A., 1996a. Syn-rift evolution of the Pripyat Trough: constraints from structural and stratigraphic modelling. Tectonophysics 268, 221–236.

Kusznir, N.J., Stovba, S.M., Stephenson, R.A., Poplavsky, K.N., 1996b. The formation of the NW Dniepr–Donets Basin: 2D forward and reverse syn-rift and post-rift modelling. Tectonophysics 268, 237–255.

Lyashkevich, Z.M., 1987. Magmatism of the Pripyat–Dnieper–Donets Paleorift (in Russian). Naukova Dumka, Kiev. 176 pp.

Mackenzie, A.S., 1984. Applications of biological markers in petroleum geochemistry. In: Brooks, J., Welte, D.H. (Eds.), Advances in Petroleum Geochemistry, vol. 1. Academic Press, London, pp. 115–214.

Mackenzie, A.S., McKenzie, D.P., 1983. Aromatization and isomerization of hydrocarbons in sedimentary basins formed by extension. Geol. Mag. 120, 417–470.

McKenzie, D., 1978. Some remarks on the development of sedimentary basins. Earth Planet. Sci. Lett. 40, 25–32.

Mello, U.T., Karner, G.D., Anderson, R.N., 1995. Role of salt in restraining the maturation of subsalt source rocks. Mar. Pet. Geol. 12, 697–776.

Milanovsky, E.E., 1992. Aulacogens and aulacogeosynclines: regularities in setting and evolution. Tectonophysics 215, 55–68.

Peters, K.E., 1986. Guidelines for evaluating petroleum source rock using programmed pyrolysis. Am. Assoc. Pet. Geol. Bull. 70, 318–329.

Poplavskii, K.N., Podladchikov, Yu.Yu., Stephenson, R.A., 2001. 2D inverse modeling of sedimentary basin subsidence. J. Geophys. Res. 106 (B4), 6657–6672.

Privalov, V.A., Panova, E.A., Azarov, N.Ya., 1998. Tectonic events in the Donets Basin: spatial, temporal and dynamic aspects (in Russian). Geol. Geochem. Foss. Fuel Depos. 4, 11–18.

Rullkötter, J., Marzi, R., 1988. Natural and artificial maturation of biological markers in a Toarcian shale from northern Germany. Org. Geochem. 13, 639–645.

Sachsenhofer, R.F., 1999. Thermal History of Well Suhadol 3. Unpubl. report, University of Leoben. 3 pp.

Sachsenhofer, R.F., Privalov, V.A., Zhykalyak, M.V., Bueker, C., Panova, E.A., Rainer, T., Shymanovskyy, V.A., Stephenson, R.A., 2002. The Donets Basin (Ukraine/Russia): coalification and thermal history. Int. J. Coal Geol. 49, 33–55.

Shpak, P.F. (Ed.), 1989. Geology and Petroleum Productivity of the Dniepr–Donetsk Depression—Petroleum Productivity (in Russian). Naukova Dumka, Kiev. 204 pp.

Starostenko, V.I., Danilenko, V.A., Vengrovitch, D.B., Kutas, R.I., Stovba, S.M., Stephenson, R.A., Kharitonov, O.M., 1999. A new geodynamical–thermal model of rift evolution, with application to the Dnieper–Donets Basin Ukraine. Tectonophysics 313, 29–40.

Stephenson, R.A., Wilson, B.M., de Boorder, H., Starostenko, V.I. (Eds.), 1996. EUROPROBE Intraplate Tectonics and Basin Dynamics of the East-European Platform. Tectonophysics, vol. 268. 309 pp.

Stephenson, R.A., Wilson, B.M., Starostenko, V.I. (Eds.), 1999. EUROPROBE Intraplate Tectonics and Basin Dynamics of the East-European Platform, vol. 2. Tectonophysics, vol. 313 414 pp.

Stephenson, R.A., Stovba, S.M., Starostenko, V.I., 2001. Pripyat–Dniepr–Donets Basin: implications for dynamics of rifting and the tectonic history of the northern Peri-Tethyan platform. In: Ziegler, P.A., Cavazza, W., Robertson, A.H.F., Crasquin-Soleau, S. (Eds.), Peri-Tethyan Rift/Wrench Basins and Passive Margins, Peri-Tethys Memoir 6. Mémoires du Muséum National d'Histoire Naturelle, vol. 186, pp. 369–406.

Stovba, S.M., Stephenson, R.A., 1999. The Donbas Foldbelt: its relationships with the uninverted Donets segment of the Dniepr–Donets Basin, Ukraine. Tectonophysics 313, 59–83.

Stovba, S.M., Stephenson, R.A., 2003. Style and timing of salt tectonics in the Dniepr–Donets Basin (Ukraine): implications for triggering and driving mechanisms of salt movement in sedimentary basins. Mar. Pet. Geol. 19, 1160–1189.

Stovba, S., Stephenson, R.A., Kivshik, M., 1996. Structural features and evolution of the Dnieper–Donets Basin Ukraine, from regional seismic reflection profiles. Tectonophysics 268, 127–147.

Sweeney, J.J., Burnham, A.K., 1990. Evaluation of a simple model of vitrinite reflectance based on chemical kinetics. Am. Assoc. Pet. Geol. Bull. 74, 1559–1570.

Taylor, G.H., Teichmüller, M., Davis, A., Diessel, C.F.K., Littke, R., Robert, P., 1998. Organic Petrology. Gebrüder Borntraeger, Berlin. 704 pp.

Ulmishek, G.F., Bogino, V.A., Keller, M.B., Poznyakevich, Z.L., 1994. Structure, stratigraphy, and petroleum geology of the Pripyat and Dniepr–Donets basins. In: Landon, S.M. (Ed.), Byelarus and Ukraine Interior Rift Basins. Am. Assoc. Pet. Geol., Mem., vol. 59, pp. 125–156.

van Wees, J.D., Stephenson, R.A., Stovba, S.M., Shymanovskyi, V.A., 1996. Tectonic variation in the Dniepr–Donets Basin from automated modelling of backstripped subsidence curves. Tectonophysics 268, 257–280.

Vitenko, V.A., Vitrik, S.P., Demyanchuk, V.G., Klitochenko, I.F., Melikov, V.A., Savchenko, V.I., Savchenko, N.I., Tsypko, A.K., Shpak, P.F., 1970. Formation and Location of Oil and Gas Deposits of the Dniepr–Donets Depression (in Russian). Tekhnika, Kyiv. 184 pp.

Wilson, M., Lyashkevich, Z.M., 1996. Magmatic evolution and the geodynamics of rifting in the Pripyat–Dniepr–Donets rift. Tectonophysics 268, 65–81.

Wygrala, B.P., 1988. Integrated computer-aided basin modelling applied to analysis of hydrocarbon generation history in a northern Italian oil field. Org. Geochem. 13, 187–197.

Yalcin, M.N., Littke, R., Sachsenhofer, R.F., 1997. Thermal history of sedimentary basins. In: Welte, D.H., Horsfield, B., Baker, D.R. (Eds.), Petroleum and Basin Evolution. Springer, Berlin, pp. 73–167.